Available online at www.sciencedirect.com

ScienceDirect

Procedia CIRP 110 (2022) 350–355

www.elsevier.com/locate/procedia

V CIRP Conference on Biomanufacturing

Preliminary tests on PEG-based thermoresponsive polymers for the production of 3D bioprinted constructs

Silvia Santoni*[a,b], Mattia Sponchioni[b], Simone Giovanni Gugliandolo[a,b], Bianca Maria Colosimo[a], Davide Moscatelli[b]

[a]*Department of Mechanical Engineering, Politecnico di Milano, Via La Masa, 1, 20156, Milano, Italy*
[b]*Department of Chemistry, Materials and Chemical Engineering "Giulio Natta", Politecnico di Milano, Piazza Leonardo da Vinci, 32, 20133, Milano, Italy*

* Corresponding author. *E-mail address:* silvia.santoni@polimi.it

Abstract

In the last years, the growing demand for tissues and organs led to the development of novel techniques, such as 3D bioprinting. This technique proved to be promising for both patient-specific and custom-made applications when using autologous cells, and for the creation of standardized models that in the future could be used for instance for high-throughput drug screening. Within this context, the formulation of bioinks that could provide reliable, reproducible, and replicable structures with good mechanical properties and high biocompatibility is a crucial challenge. In this work, the use of a thermoresponsive PEG-based formulation was investigated as a bioink, allowing its use for 4D bioprinting applications triggered by thermal changes. First, the polymer was synthesized by reversible addition-fragmentation chain transfer polymerization (RAFT), which allows for optimal control over the final properties of the polymer. Then, the printability for extrusion-based bioprinting of this formulation was assessed through in-situ imaging. Finally, the use of this polymer as bioink was tested by encapsulation of endothelial cells and evaluating cell distribution within the construct.

Keywords: 3D bioprinting; printability; endothelial cells; thermoresponsive polymers; bioink

Nomenclature

NMR	Nuclear Magnetic Resonance
2PP	2-Photon Polymerization
CPA	4-Cyano-4-(phenylcarbonothioylthio)pentanoic acid
DLS	Dynamic Light Scattering
DP	Degree of Polymerization
EG2MA	Di(ethylene glycol) methyl ether methacrylate
LCST	Lower Critical Solution Temperature
mCTA	Macro Chain Transfer Agent
PEG	Poly(ethylene glycol)
PR	Printability
RAFT	Reversible Addition-Fragmentation chain Transfer polymerization
RGD	Arg-Gly-Asp
T_{CP}	Cloud point temperature
UCST	Upper Critical Solution Temperature

1. Introduction

3D bioprinting is a promising technique that enables the production of cellularized constructs in complex and predefined 3D shapes[1,2]. One of the key elements of this technique is the bioink, which contains the cells and works as a structural element that provides the cells with the required mechanical support for them to grow and proliferate in the desired conformation[3]. This component is typically a polymeric material in the form of hydrogels, mainly due to their biocompatibility, high water content, and

2212-8271
10.1016/j.procir.2022.06.062

biodegradability[4,5]. In the literature, various materials have been investigated for 3D bioprinting, characterized by peculiar properties depending on the technique used (i.e. extrusion, inkjet, laser-assisted, stereolithography, and 2PP) and the application[6].

In the last years, stimuli-responsive polymers have been gaining attention to encounter the need for applications of increased complexity in what is now called 4D bioprinting, where the construct changes dynamically in time in response to environmental stimuli. Examples of materials belonging to this category are thermoresponsive materials, pH-responsive materials, and enzyme-responsive materials[7]. Among these, thermoresponsive polymers are the most studied and indeed the most versatile. This is due to the easiness of application of thermal stimuli and hence to induce their reversible phase transition[8]. Depending on their behavior, thermoresponsive polymers can show a lower critical solution temperature (LCST) or an upper critical solution temperature (UCST). Particularly relevant for 3D bioprinting are those thermoresponsive polymer formulations engineered to go from free-flowing liquids to self-standing gels when the temperature is raised above their cloud point (T_{cp}). In fact, this peculiar behavior allows the curing of the bioink after printing and the formation of the 3D construct through mild and non-invasive heating.

In 3D bioprinting and more broadly on biofabrication, they are exploited as i) bioinks, ii) biomaterials for scaffold production, iii) sacrificial or fugitive inks. In the first case, they are used as bioinks when directly mixed with cells. Conversely, they can be used to produce scaffolds if the cells are seeded on top after the printing process. Thanks to their responsive behavior, they are often used as fugitive inks without inks to indirectly produce shapes. This is particularly useful to produce vascularized structures. In this case, thermoresponsive polymers are printed together with a stable bioink, which is crosslinked and followed by the solubilization and removal of the fugitive ink. Other types of applications in biofabrication are for instance their use to produce cell sheets, when they are used as coatings and after a cell monolayer is formed the sol-gel transition is exploited to safely retrieve the cell layer. Most of the studied thermoresponsive polymers present in the literature for 3D bioprinting are used in extrusion-based bioprinting[9].

A wide variety of thermoresponsive polymers are now available, from natural to synthetic ones. Natural polymers are characterized by high biocompatibility due to the presence of cell-binding motifs, but they usually show variability from batch to batch and poor mechanical properties. On the contrary, synthetic polymers are highly replicable and their formulation can be tuned to modulate their degradation rates and mechanical properties.[10] However, they are still less commonly used mainly due to the absence of cell binding sites. This limitation is being overcome by functionalizing the polymers with cell-binding motifs (e.g., oligopeptides such as Arg-Gly-Asp motif - RGD) and growth and differentiation factors to favor cell interaction and proliferation[10].

Some examples of natural thermoresponsive bioinks are agarose, methyl cellulose[11], gelatin, and collagen[12,13]. The first two are plant-based polysaccharides and they do not exhibit cell-interacting sites. The latter two are polypeptides obtained from animal origin; they are related in terms of composition because gelatin is formed from the hydrolysis of collagen. They are often used because of their biomimicry and the presence of cell anchoring motifs.

Classes of synthetic polymers already used in 3D bioprinting are i) poloxamers, ii) poly(N-isopropylacrylamide), iii) PEG-based thermoresponsive polymers, iv) poly(2-oxazoline)/poly(2-oxazine), v) elastin-like polypeptides (ELPs), vi) PIC. Most of these classes are starting to be investigated to form composites when added with nanoclays (e.g. laponite[14,15]), hydroxyapatite[16,17], and graphene[18], to improve their printability and functionality, materials such as can be added to the hydrogels to form composites.

Poloxamers are one of the most common classes of synthetic and now commercially available thermoresponsive polymers. In particular, Pluronic F127 is widely used both as bioink and fugitive ink in biofabrication. Examples of its use as bioink include the bioprinting of fibroblasts[19] and chondrocytes[20]. In some cases, it is combined with alginate for bioprinting of hepatocytes [21], myoblasts to study their differentiation[22]. The quick degradation rate of Pluronic makes it not suitable for long term cell viability studies[19] but this has been overcome by its mixing with diacrylates and subsequent UV crosslinking and tested for bioprinting of chondrocytes[20]. An example of Pluronic use as sacrificial ink is in combination with agarose to use if for the production of sacrificial molds[23].

Poly(N-isopropylacrylamide) or PNIPAAm is a versatile polymer frequently used for biomedical applications. In 3D bioprinting they have been used as bioinks, biomaterials for scaffold preparation, and sacrificial inks. For instance, they were used in combination with hyaluronan and methacrylated hyaluronan to produce scaffolds where chondrocytes were seeded and cultured[24]. It was also included in a glucose-sensitive formulation in combination with pentafluorophenyl acrylate and poly(vinyl alcohol)[25].

Polymers based on PEG are of particular interest because of their non-toxicity and the fact that they are FDA approved.[26] Relative to the bioprinting field, pHMA-lac-PEG polymers have been used for instance in combination with chondroitin sulfate for the bioprinting of chondrocytes for cartilage tissue engineering[27,28].

Poly(2-oxazoline)/poly(2-oxazine) (pOx/pOzi) have been investigated as bioink alone or mixed with alginate to bioprint fibroblast or in combination with laponite to bioprint adipose stem cells, showing good printability[15].

Elastin-like peptides (ELPs) have been studied very recently in the field of 3D bioprinting and they proved to be promising for their use with fibroblasts, endothelial cells, and mesenchymal stem cells[29].

Another synthetic thermoresponsive material which is starting to gain attention in 3D bioprinting is polyisocyanide (PIC), which is interesting because of its transition temperature close to the physiological one (37°C). PIC has been employed as sacrificial material and its printability has been evaluated in absence of cells[30].

As mentioned above, some examples of PEG-based thermoresponsive polymers have been investigated. However, their printability was still not investigated thoroughly. In this work, we developed a synthetic thermoresponsive polymer based on polyethylene glycol (PEG) that can undergo a reversible formation of a self-standing gel by mild heating at T>26 °C. The peculiar comb-like microstructure of the polymer

allows tuning important parameters, including the molecular weight and its rheology. As such, after proper characterization of the produced material, we demonstrate how it can be advantageously exploited as a bioink in the extrusion 3D bioprinting of human umbilical vein endothelial cells (HUVEC).

2. Materials and methods

2.1. Materials

For the polymer synthesis, poly(ethylene glycol) methyl ether ($mPEG_{113}$, average Mn=5000, Sigma Aldrich), 4-Cyano-4-(phenylcarbonothioylthio)pentanoic acid (CPA, ≥ 97%, Sigma Aldrich), di(ethylene glycol) methyl ether methacrylate (EG2MA, 95%, MW=188.22, Sigma Aldrich), n-hexane (≥ 99%, MW=86.18, Sigma Aldrich), ethyl acetate (pure, MW=88.11, Carlo Erba), 2,2′-Azobis(2-methylpropionamidine) dihydrochloride (α-α, MW= 271.19, Sigma Aldrich), phosphate buffered saline (PBS, Sigma Aldrich), dichloromethane (DCM, ≥99%, Fisher Chemical), deuterochloroform (CDCl3, 99.8%, MW=120.38, Sigma-Aldrich), were used as received except when specifically noted. All the solvents used were of analytical purity and used as received.

2.2. Polymer synthesis and characterization

Prior to synthesis, 10g of EG2MA monomer was purified using a Biotage Isolera flash chromatography equipped with a Biotage Snap Ultra 100g silica chromatographic column with a method based on a gradient of n-hexane (A) and ethyl acetate (B) as solvents. First, the column was equilibrated with a ratio A/B=10-11% for 1 column volume (CV) with a flowrate of 100 mL/min. Retardation factors (Rf) were set to 0.25 and 0.75 for the impurities and the product, respectively. The method included a first step with a solvent ratio of A/B kept constant for 1 CV, followed by a gradient from 11% to 80% over 10 CV. UV signals were measured at 219 nm and 350 nm for the collection and the threshold for collecting was set to 400 mAU. The fractions containing the impurities were discharged and solvents were removed from the product through vacuum evaporation.

The polymer $mPEG_{113}$-$EG2MA_{700}$-CPA was synthesized via reversible addition-fragmentation chain transfer polymerization (RAFT). The $mPEG_{113}$-CPA (macro chain transfer agent, macroCTA) was synthetized according to Sponchioni et al.[31] In brief, $mPEG_{113}$ was functionalized in a first intermediate with methanesulfonyl chloride (OMS), forming $mPEG_{113}$-OMS. After this, the mesylate was removed through nucleophilic substitution with ammonia, forming the second intermediate $mPEG_{113}$-NH_2. CPA-NHS was formed from CPA and NHS exploiting DCC/DCM chemistry. $mPEG_{113}$-NH_2 and CPA-NHS were dissolved in DCM and the first solution was added dropwise to the second one and later concentrated to obtain the product $mPEG_{113}$-CPA. The macroCTA was used to synthetize the macroCTA-$EG2MA_{700}$ polymer by adding purified EG2MA to reach a theoretical DP of 700 ([EG2MA]/[macroCTA]=700), initiator ([I]/[macroCTA]=1/3), and deionized water solvent to a final desired polymer concentration of 15% w/w. The solution was filtered through a 0.2 mm filter for sterilization and the reaction was left to occur for 24 h at 50 °C.

Polymer composition was assessed through nuclear magnetic resonance (^{1}H-NMR) analysis. For a visual verification of the polymer ability to thermally crosslink, tube inversion test was performed. After that, the T_{cp}^{LCST} was measured through dynamic light scattering analysis (DLS) with a Zetasizer Nano ZS (Malvern Instrument), relying on the formation of scattering centers and particle increase in size after the sol-gel transition. For the analysis, samples were diluted to a final concentration of 0.5% w/w. Temperature ramps were performed in a range from 20°C to 30°C. After setting an increase of temperature of 1°C, the samples were equilibrated for 300 s. The measure was repeated three times. The T_{cp}^{LCST} was obtained as the inflection point of the sigmoidal curve of the particle dimension versus temperature.[32]

2.3. Extrusion 3D bioprinting

3D bioprinting was performed using a pneumatic extrusion-based bioprinter (BioX, CELLINK, Gothenburg, Sweden). In all the experiments, the hydrogel was loaded into a 3 ml cartridge and centrifuged to remove air bubbles. A sterile 22G (0.410 mm) conical nozzle was used, setting a 0.2 mm offset. The temperature of the printbed was set to 35 °C and the temperature-controlled printhead to 20 °C. The pressure was set in a range 3-7 kPa and printing speed in a range of 15-25 mm/s(Table 1). Co-axial in situ images were acquired after the printing of every layer using the BioX HD integrated camera and analyzed using custom-made MATLAB® R2021a (MathWorks, Natick, USA) scripts.

Table 1. Optimal printing parameters for this formulation.

Material	Pressure (kPa)	Velocity (mm/s)	Printbed temperature (°C)	Printhead temperature (°C)
macroCTA-$EG2MA_{700}$	3	20	35	20
macroCTA-$EG2MA_{700}$	5	15	35	20

2.4. Cell encapsulation and imaging

Endothelial HUVEC cells were cultured in complete medium Endothelial Cell Growth Medium (PromoCell) in t75 flasks. Prior to 3D bioprinting, cells were stained using a red fluorescent vital dye (CellTracker™ Red CMTPX Dye, Invitrogen) according to the manufacturer's instructions. After detachment through trypsinization, cells were counted, and cell viability was assessed using Trypan blue solution 0.4% in a concentration 1:1 v/v using a microscope (Celena S, Logos Biosystems). An appropriate volume of cell suspension to obtain the required number of cells was centrifuged at 220 rpm for 3 minutes at 37°C and the pellet was resuspended and mixed with the hydrogel to form the bioink. The constructs were

analyzed through fluorescence imaging using a fluorescence microscope (Celena S, Logos Biosystems).

3. **Results and discussion**

First, the thermoresponsive polymer intended to be used as bioink was synthetized via reversible addition-fragmentation chain transfer (RAFT) polymerization. A $mPEG_{113}$-CPA (macroCTA) was chain extended with EG2MA targeting a degree of polymerization (DP) of 700 and a final concentration of 15% w/w (macroCTA-$EG2MA_{700}$, Fig. 1.a). The composition of the obtained polymer was evaluated through

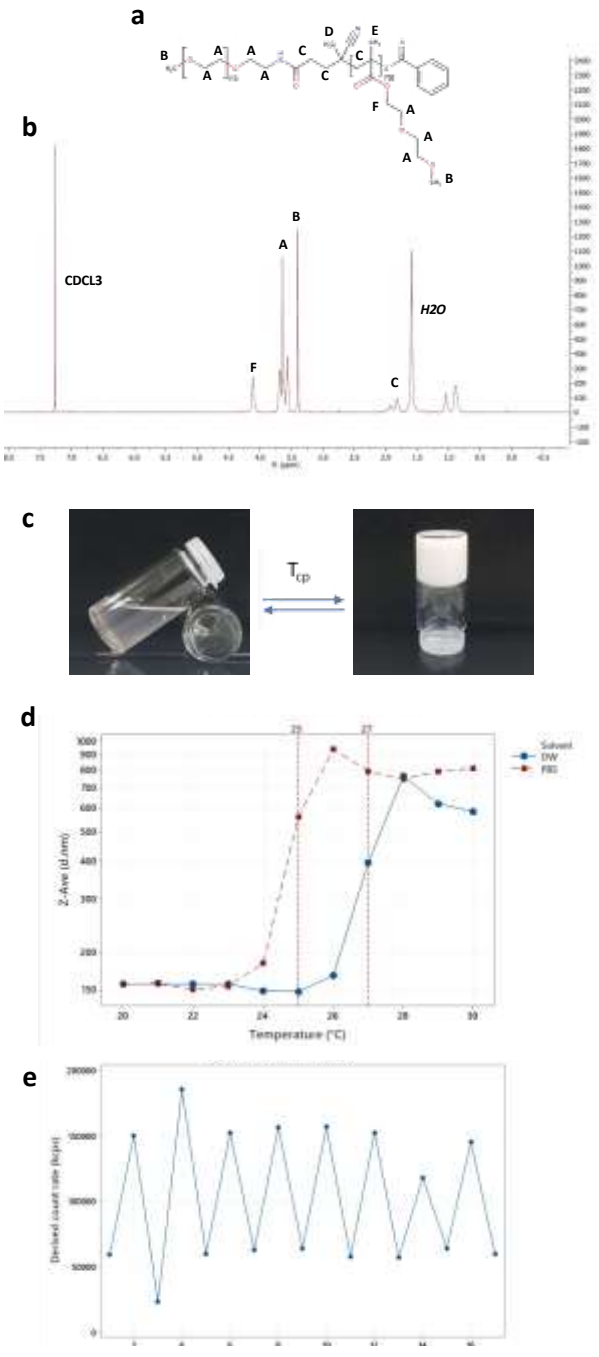

Fig. 1. Polymer characterization. (a) Structure of the polymer macroCTA-$EG2MA_{700}$; (b) ^{1}H-NMR characterization of the polymer; (c) inversion test; (d) transition temperature in deionized water and PBS as solvents obtained from DLS measurements; (e) reversibility of the transition: multiple cycles of heating and cooling were performed while the transition still occurred.

^{1}H-NMR spectroscopy (Fig. 1.b). This confirmed an almost complete monomer conversion after 24 h and the desired chain length. The possibility of obtaining a thermally induced sol-gel transition was assessed through inversion tube test (Fig. 1.c). In particular, the formulation behaved as a flowing liquid at T = 4 °C, while turned to a self-standing gel once heated to 30 °C. The precise transition temperature T_{cp}^{LCST} was assessed through DLS measurements aimed at tracking the average nanoparticle size at increasing temperature. This markedly increased past the cloud point, which was considered as the inflection point of the size vs temperature curves. In particular, a T_{cp}^{LCST} =27°C was obtained in deionized water and a T_{cp}^{LCST} =25°C was measured in presence of PBS as solvent (Fig. 1.d). This behavior was expected in presence of ions which favor the salting out of the solvent and subsequent precipitation. The reversibility of the transition was confirmed repeating multiple cycles of equilibration at temperature lower than the T_{cp}^{LCST} (20°C) and higher than the T_{cp}^{LCST} (30°C) (Fig. 1.e).

To evaluate the possible use of this thermoresponsive hydrogel for extrusion bioprinting, 3D bioprinted constructs were produced. To achieve good printability, the polymer should be printed at low viscosity and kept at a temperature below the T_{cp}^{LCST}, but the sol-gel transition should occur as soon as it is extruded. This can be induced by heating the build plate. The quality of the printed construct was assessed by measuring the filament regularity and the printability of grid constructs. Printability (Pr) of the grid constructs printed using the optimal parameters obtained from checking the filament regularity was assessed following the equation as previously defined in the literature:

$$Pr = \frac{L^2}{16A}$$

Where L is the perimeter of the pore and A the area of the pore.[33]–[36] L and A were measured by image analysis through a MATLAB® script where segmentation based on k-means algorithm was followed by the analysis of connected components. The closer *Pr* to 1, the better. In Fig. 2, the printability and the area of the pore of a construct made of 5 layers are shown. The measures are in accordance with the visual evaluation of the samples, where a worsening of the printability can be observed after the first layers, as well as a reduction in the area of the pore up to the disappearance of the pore in some cases after the fourth layer. The printability within a cellularized construct was also investigated (Fig. 3). In both cases, the average printability Pr obtained for our formulation (5 layers grid: i. 0.93±0.01, ii. 1.30±0.11, iii. 1.21±0.09; 1 layer grid 20x20x0,3 mm: 1.25±0.20) is comparable with others found in the literature[7].

After the printability assessment, the polymer was tested for its suitability for usage as a bioink. Cell-laden constructs encapsulating HUVEC were produced. The cells were mixed with the ink at a temperature below the T_{cp}^{LCST}, exploiting the low viscosity of the liquid formulation. The thermal crosslink was induced after extrusion by heating the build plate above the T_{cp}^{LCST}. HUVEC were cultured in complete culture medium (Endothelial Growth Medium, PromoCell). For cell

identification in the construct, cells were pre-stained using a non-destructive cell staining method fluorescent in red (Fig. 4). After incubation with the dye, cells were detached by trypsinization. Cell number and viability of cells in suspension were measured via Trypan Blue exclusion. After that, cells were centrifuged for 3 minutes at 220 rpm, the pellet was resuspended and mixed with the thermoresponsive polymer 15% w/w to a final concentration of $2.5*10^6$ cell/ml.

After 3D bioprinting, the constructs were submerged in pre-warmed culture medium and incubated at 37°C. To investigate cell distribution within the construct, bright field and fluorescent images were acquired using a fluorescent microscope (Celena S). Afterwards, cell positioning and number were evaluated through a custom-made algorithm on MATLAB® based on the dimension and roundness of the spot (Fig. 4.b,c). Uniform cell distribution can be achieved thanks to the low viscosity of the hydrogel in the liquid form during the mixing and extrusion of the bioink at a temperature lower than the T_{cp}^{LCST}.

Overall, the developed thermoresponsive material demonstrated good potential as a bioink for extrusion 3D bioprinting, bringing about the possibility of a uniform mixing with the cells and the non-invasive curing allowing the formation of cellularized 3D constructs.

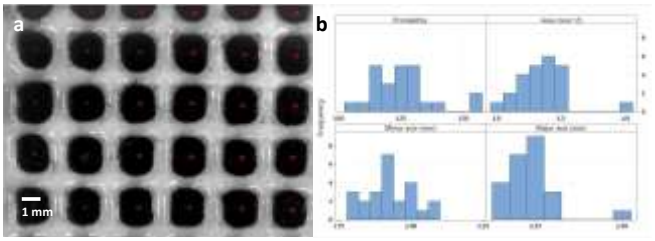

Fig. 3. Printability within a construct. (a) A cellularized construct of 20x20x0.3 mm was printed using a conical 22G nozzle and an offset of 0.2 mm. HUVEC cells were encapsulated in this case to a final concentration of $2.5*10^6$ cells/ml. (b) Measures relative to printability (Pr=1.2486±0.1213), area (A=3.3±0.2 mm^2), maximum (Max_axis=2.2±0.1 mm) and minor axis (Min_axis=1.9±0.1 mm) of the pore obtained through image analysis are shown. Pores whose images were cropped (first row) are not represented in (b).

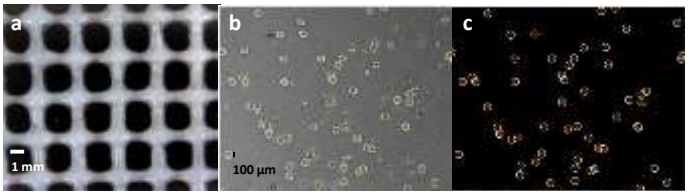

Fig. 4. 3D bioprinting of a cell-laden construct. (a) in situ images of the 3D bioprinted construct acquired immediately after the printing process. (b,c) ex situ images of the construct after one hour of incubation in culture medium. b) 4x bright-field image, c) fluorescently labeled cells. Cell number and positioning within the construct were analyzed from fluorescent images through a custom-made MATLAB® algorithm (e.g. in this image, 57 cells could be counted). The yellow circles represent the spot identified within the image where cells are present.

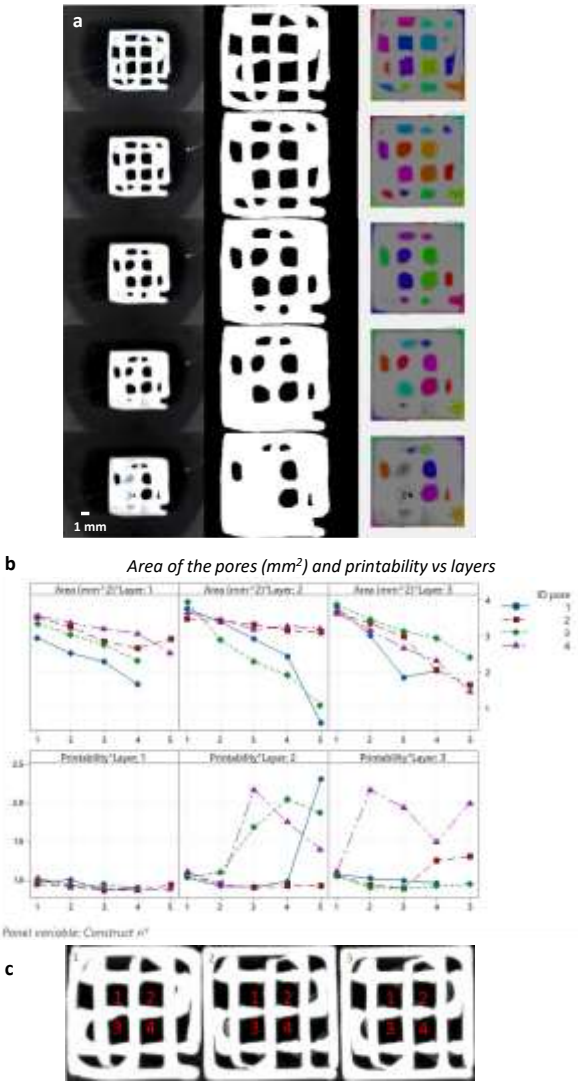

Fig. 2. Printability over the layers. A construct of 10x10x2mm was printed using a conical 22G nozzle and 0.2 mm of offset. For each of the three replicates, data about the four central pores are presented. (a) In situ images of each layer of the construct, binarization to obtain the shape of the last layer, labeling of the pores over the 5 layers. (b) Area in mm^2 and printability Pr over the layers of each one of the four central pores. The panels represent three different constructs; on the x axis, the 5 layers are shown. On the y axis, area and printability are shown. (c) Images of the first layers of the constructs.

4. Conclusions

This work is meant as a proof of concept of the use of PEG-based thermoresponsive polymers as bioink for 4D bioprinting. Compared to other polymerization mechanisms, RAFT polymerization allows for high replicability and reproducibility of the obtained polymer in terms of DP and molecular weight. Moreover, it opens the possibility of finely modulating the polymer properties and functionalization. The developed polymers allow good printing accuracy achieved thanks to the quick crosslinking kinetics. The on-off behavior of the polymer can be activated in a small interval of temperature (less than 3°C) close to the physiological one. This characteristic coupled with the low viscosity of the ink below the LCST and its shear-thinning behavior allows to reduce the shear stress applied on the cells. Moreover, the possibility of curing the bioink by mild heating at 37 °C prevents thermal stresses on the cells. These preliminary results confirm the potentiality of this type of polymers in advanced 3D bioprinting.

5. References

[1] Choudhury, D., Anand, S., and Naing, M. W. The arrival of commercial

bioprinters - Towards 3D bioprinting revolution!. Int. J. Bioprinting 2018; 4(2).
[2] Santoni, S., Gugliandolo, S. G., Sponchioni, M., et al. 3D bioprinting: current status and trends—a guide to the literature and industrial practice. Bio-Design Manuf. 2021; 5(1):14–42.
[3] Groll, J., Burdick, J. A., Cho, D.-W., et al. A definition of bioinks and their distinction from biomaterial inks. Biofabrication 2018; 11(1):013001.
[4] Sears, N. A., Seshadri, D. R., Dhavalikar, P. S., et al. A Review of Three-Dimensional Printing in Tissue Engineering. Tissue Eng. - Part B Rev. 2016; 22(4):298–310.
[5] Gungor-Ozkerim, P. S., Inci, I., Zhang, Y. S., et al. Bioinks for 3D bioprinting: An overview. Biomater. Sci. 2018; 6(5):915–946.
[6] Li, J., Chen, M., Fan, X., et al. Recent advances in bioprinting techniques: Approaches, applications and future prospects. J. Transl. Med. 2016; 14(1):271.
[7] Fu, Z., Ouyang, L., Xu, R., et al. Responsive biomaterials for 3D bioprinting: A review. Mater. Today 2022; xxx(xx).
[8] Sponchioni, M., Capasso Palmiero, U., and Moscatelli, D. Thermo-responsive polymers: Applications of smart materials in drug delivery and tissue engineering. Mater. Sci. Eng. C 2019; 102(February):589–605.
[9] Suntornnond, R., An, J., and Chua, C. K. Bioprinting of Thermoresponsive Hydrogels for Next Generation Tissue Engineering: A Review. Macromol. Mater. Eng. 2017; 302(1).
[10] Sponchioni, M., Manfredini, N., Zanoni, A., et al. Readily Adsorbable Thermoresponsive Polymers for the Preparation of Smart Cell-Culturing Surfaces on Site. ACS Biomater. Sci. Eng. 2020; 6(9).
[11] Bonetti, L., De Nardo, L., and Farè, S. Thermo-Responsive Methylcellulose Hydrogels: From Design to Applications as Smart Biomaterials. Tissue Eng. - Part B Rev. 2021; 27(5):486–513.
[12] Cao, H., Duan, L., Zhang, Y., et al. Current hydrogel advances in physicochemical and biological response-driven biomedical application diversity. Signal Transduct. Target. Ther. 2021; 6(1):1–31.
[13] Willson, K., Atala, A., and Yoo, J. J. Bioprinting au natural: The biologics of bioinks. Biomolecules 2021; 11(11).
[14] Hu, C., Haider, M. S., Hahn, L., et al. Development of a 3D printable and highly stretchable ternary organic-inorganic nanocomposite hydrogel. J. Mater. Chem. B 2021; 9(22):4535–4545.
[15] Haider, M. S., Ahmad, T., Yang, M., et al. Tuning the thermogelation and rheology of poly(2-oxazoline)/poly(2-oxazine)s based thermosensitive hydrogels for 3d bioprinting. Gels 2021; 7(3).
[16] Chen, Y. Y., Li, H. L., Chen, C. C., et al. Biofabrication of biopolymer and biocomposite scaffolds for bone tissue engineering. Key Eng. Mater. 2012; 523–524:374–379.
[17] Ji, X., Yuan, X., Ma, L., et al. Mesenchymal stem cell-loaded thermosensitive hydroxypropyl chitin hydrogel combined with a three-dimensional-printed poly(ε-caprolactone) /nano-hydroxyapatite scaffold to repair bone defects via osteogenesis, angiogenesis and immunomodulation. Theranostics 2020; 10(2):725–740.
[18] Wang, J., Xia, Z., Liu, J., et al. Facile fabrication of near-infrared light-responsive shape memory nanocomposite scaffolds with hierarchical porous structures. J. Appl. Polym. Sci. 2021; 138(37):1–14.
[19] Gioffredi, E., Boffito, M., Calzone, S., et al. Pluronic F127 Hydrogel Characterization and Biofabrication in Cellularized Constructs for Tissue Engineering Applications. Procedia CIRP 2016; 49(iii):125–132.
[20] Müller, M., Becher, J., Schnabelrauch, M., et al. Nanostructured Pluronic hydrogels as bioinks for 3D bioprinting. Biofabrication 2015; 7(3).
[21] Gori, M., Giannitelli, S. M., Torre, M., et al. Biofabrication of Hepatic Constructs by 3D Bioprinting of a Cell-Laden Thermogel: An Effective Tool to Assess Drug-Induced Hepatotoxic Response. Adv. Healthc. Mater. 2020; 9(21).
[22] Mozetic, P., Giannitelli, S. M., Gori, M., et al. Engineering muscle cell alignment through 3D bioprinting. J. Biomed. Mater. Res. - Part A 2017; 105(9):2582–2588.
[23] Müller, M., Becher, J., Schnabelrauch, M., et al. Printing thermoresponsive reverse molds for the creation of patterned two-component hydrogels for 3D cell culture. J. Vis. Exp. 2013; 99(77):1–9.
[24] Kesti, M., Müller, M., Becher, J., et al. A versatile bioink for three-dimensional printing of cellular scaffolds based on thermally and photo-triggered tandem gelation. Acta Biomater. 2015; 11(1):162–172.
[25] Tsai, Y. L., Theato, P., Huang, C. F., et al. A 3D-printable, glucose-sensitive and thermoresponsive hydrogel as sacrificial materials for constructs with vascular-like channels. Appl. Mater. Today 2020; 20:100778.
[26] Ozbolat, I. T. and Hospodiuk, M. Current advances and future perspectives in extrusion-based bioprinting. , Biomaterials. 2016.
[27] Abbadessa, A., Mouser, V. H. M., Blokzijl, M. M., et al. A Synthetic Thermosensitive Hydrogel for Cartilage Bioprinting and Its Biofunctionalization with Polysaccharides. Biomacromolecules 2016; 17(6):2137–2147.
[28] Mouser, V. H. M., Abbadessa, A., Levato, R., et al. Development of a thermosensitive HAMA-containing bio-ink for the fabrication of composite cartilage repair constructs. Biofabrication 2017; 9(1).
[29] Salinas-Fernández, S., Santos, M., Alonso, M., et al. Genetically engineered elastin-like recombinamers with sequence-based molecular stabilization as advanced bioinks for 3D bioprinting. Appl. Mater. Today 2020; 18:100500.
[30] Celikkin, N., Padial, J. S., Costantini, M., et al. 3D printing of thermoresponsive polyisocyanide (PIC) hydrogels as bioink and fugitive material for tissue engineering. Polymers (Basel). 2018; 10(5).
[31] Sponchioni, M., O'Brien, C. T., Borchers, C., et al. Probing the mechanism for hydrogel-based stasis induction in human pluripotent stem cells: Is the chemical functionality of the hydrogel important?. Chem. Sci. 2020; 11(1):232–240.
[32] Chandrasiri, I., Abebe, D. G., Gupta, S., et al. Synthesis and characterization of polylactide-PAMAM "Janus-type" linear-dendritic hybrids. J. Polym. Sci. Part A Polym. Chem. 2019; 57(13):1448–1459.
[33] Uzun-Per, M., Gillispie, G. J., Tavolara, T. E., et al. Automated Image Analysis Methodologies to Compute Bioink Printability. Adv. Eng. Mater. 2021; 23(4):1–12.
[34] Schwab, A., Levato, R., D'este, M., et al. Printability and Shape Fidelity of Bioinks in 3D Bioprinting. 2020.
[35] Strauß, S., Meutelet, R., Radosevic, L., et al. Printability in extrusion bioprinting. Biofabrication 2021; 12(3):11028–11055.
[36] Gillispie, G., Prim, P., Copus, J., et al. Assessment methodologies for extrusion-based bioink printability. Biofabrication 2020; 12(2).